

Structural Analysis and Characterization of Cu, Sr-doped Hydroxyapatite Whiskers

Ying Guo¹, Jin Wen^{1,2,a}, Hongquan Zhang^{1,2,b}, Luwei Fu¹, Fei Yang¹

¹State Key Laboratory of Silicate Materials for Architecture (Wuhan University of Technology),
Wuhan 430070, China

²School of Materials Science and Engineering, Wuhan University of Technology, Wuhan 430070,
China

^awen9888@hotmail.com, ^bzhqquan@whut.edu.cn

Keywords: Cu and Sr ions; ions doping; hydroxyapatite whisker

Abstract. Cu and Sr ions doped hydroxyapatite ($\text{Ca}_{10}(\text{PO}_4)_6(\text{OH})_2$, HA) whiskers were synthesized by hydrothermal homogeneous precipitation method. The morphology, structure and the phase composites of the products were characterized by XRD, FTIR and SEM. The results showed that Cu^{2+} or Sr^{2+} partially substituted for Ca^{2+} in the HA crystal, resulting in lattice distortion and lower crystallinity with Sr or Cu addition. For Cu-doped HA (Cu-HA) whiskers, the doping limit proportion should be below 8mol%, and for Sr-doped HA whiskers (Sr-HA), it was below 20mol%.

Introduction

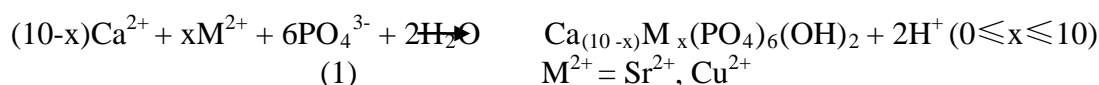
Hydroxyapatite ($\text{Ca}_{10}(\text{PO}_4)_6(\text{OH})_2$, HA) is the main inorganic component of vertebrate bones and teeth. Synthetic HA has been gradually accepted and widely used to repair bone and tooth defects due to its similarity with the composition of human hard tissue [1,2].

It was well known that most HA of natural bone is non-stoichiometric because of the presence of minor constituents, such as cations (Na^+ , Mg^{2+} , Sr^{2+} , Zn^{2+} , K^+) and anions (HPO_4^{2-} , CO_3^{2-} , Cl^-). Metal ions in bone tissue have been proven to play an active role in promoting bone mineralization and angiogenesis [3,4]. However, for the synthetic HA, only Ca, P, O and H elements remain in the crystal structure, showing a higher stability than that of natural apatite. Thus, ions doping has been attracted more attention to improve the biological behavior and clinical application of HA materials [5].

It has been showed that the presence of divalent metal ions (Mg^{2+} , Zn^{2+} , Sr^{2+}) in HA crystals not only affected their crystallization behavior, solubility and surface chemical properties, but also exerted a positive influence on the formation of bone mineral and the biological characteristics of HA materials [6-8]. Mg^{2+} doping has been confirmed to be able to regulate the formation and remodeling of bone tissue; Ren et al, reported that when the molar fraction of Zn in artificial bone was in the range of 5-20%, Zn substitution in the apatite lattice, rather than adsorption on the surfaces, and it had a direct stimulation on the growth of osteogenesis cells, while relatively inhibit the growth of osteoclast [9,10]. Comparing with pure HA, Li et al, found that 5-50 mol% Sr-doped HA had better biocompatibility and biological activity; Kim et al found that ceramics based on HA made in a wet chemical process with addition of $\text{Cu}(\text{NO}_3)_2 \cdot 3\text{H}_2\text{O}$ had good antimicrobial [11,12]. Although the effects of these metal ions doped HA on the structure, solubility and biological performance have been made in the previous studies, few literatures focus on metal ions doped HA whiskers. Therefore, effects of Sr^{2+} and Cu^{2+} doping on the structure and morphology of HA whiskers will be made in this study so as to find a reasonable doping moral proportion of Cu and Sr ions in HA crystals.

Materials and Methods

Preparation of metal ions doped HA. Metal ions doped HA whiskers were synthesized by a hydrothermal homogeneous precipitation method according to the following reaction equation [13]:



Appropriate amounts of aqueous solution containing 0.05 mol/L $\text{Ca}^{2+} + \text{M}^{2+}$ and 0.03 mol/L PO_4^{3-} were first prepared by dissolving $\text{Ca}(\text{NO}_3)_2 \cdot 4\text{H}_2\text{O}$, $\text{NH}_4\text{H}_2\text{PO}_4$, $\text{Sr}(\text{NO}_3)_2$ or $\text{Cu}(\text{NO}_3)_2 \cdot 3\text{H}_2\text{O}$ in a 250ml volumetric flask under constant stirring with teflon-coated magnetic stirring bar, in which doping proportion of Sr^{2+} was 5-40mol%, and for Cu^{2+} was 5-15mol%. 1mol/L $\text{C}_2\text{H}_5\text{NO}$ was added into the mixed solution and its pH was adjusted to 3.00 by addition of 1mol/L HNO_3 and 1:1 NH_4OH solutions under constant stirring; after the configured solution was heated at 180°C for 10-12h in a hydrothermal reactor, the precipitates were filtered with a vacuum filter, and washed three times with deionized water, finally dried at 70-80°C for 1-2h in a vacuum oven for use.

Materials characterization. Rotation Anode High Power X-ray Diffractometer (XRD) (D/MAX-RB, Rigaku Corporation, Japan) was used to analyze the phase composition of the precipitates in the range $2\theta=10-65^\circ$ with Cu $K\alpha$ radiation. The Fourier-transform infrared spectroscopy (FTIR) (FTIR, Nicolet IS10, Thermo Nicolet, USA) was recorded in the range of 4000-400 cm^{-1} to identify and analyze the functional group of the samples. Microstructural feature of the samples was observed by a Scanning Electron Microscope (SEM) (SEM, JSM-5610LV, JEOL, Japan).

Results and discussion

Sr doped HA.

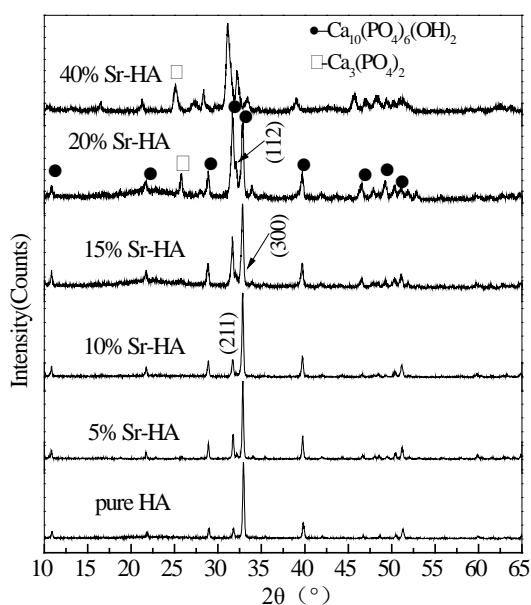


Fig.1 XRD patterns of Sr ions doped HA whiskers

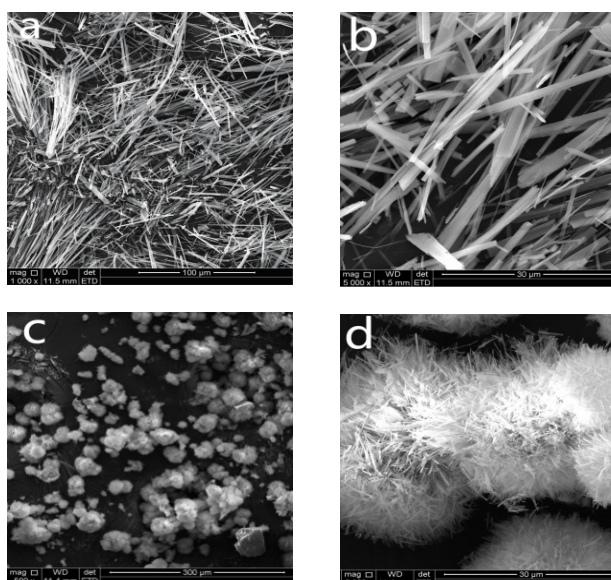


Fig.2 SEM images of Sr ions doped HA whiskers
a,b-5mol% Sr-HA c,d-20mol% Sr-HA

Fig.1 showed the XRD patterns of Sr-doped HA (Sr-HA) prepared with different molar ratio of Sr/(Ca+ Sr). For Sr doping concentration less than 20 mol%, the diffraction peaks were identified as HA, and the ratio of $I_{(300)}/I_{(211)}$ of the Sr-HA whiskers was lower than that of synthesized HA indicated in the JCPDS PDF 09-432. Because Sr^{2+} radius is bigger than Ca^{2+} radius, lattice distortion occurs when Sr^{2+} substitutes Ca^{2+} , leading to an expansion of interplanar crystal spacing (d). According to Bragg equation: $\lambda=2d\sin\theta$, when wavelength (λ) is certain, the diffraction angle (2θ) would be smaller with d spacing. Thus, increasing Sr doping concentration, the diffraction peaks shifted to

small diffraction angle comparing with pure HA. In addition, the diffraction peak for (211) obviously became stronger, while (300) became weaker, which indicated that crystal growth along *c*-axis orientation trended to become weaker. However, it was found that the second phase, assigned to tricalcium phosphate ($\text{Ca}_3(\text{PO}_4)_2$, PDF#:9-169), appeared at about $2\theta \approx 26^\circ$ when the Sr doping concentration was 20 mol%. Further increasing the Sr concentration, the diffraction peaks obvious shifted to lower diffraction angle, and the peak intensity ratio of $I_{(300)}/I_{(211)}$ greatly decreased comparing the sample doped with low Sr concentration, which indicated that the morphology of Sr-HA whiskers changed with the Sr/(Ca+Sr) doping ratio.

The morphology of Sr doped HA was showed in Fig.2. The whiskers had a needle-like morphology for 5mol% Sr-HA (Fig. 2a and 2b). However, with increasing Sr content more than 20mol%, the whiskers tended to agglomerate and the size of the whiskers became smaller and shorter (Fig. 2c and 2d), and blocky-like impurity appeared, which was mainly caused by the appearance of the second phase ($\text{Ca}_3(\text{PO}_4)_2$). This supported precisely the XRD pattern analysis results.

Cu doped HA.

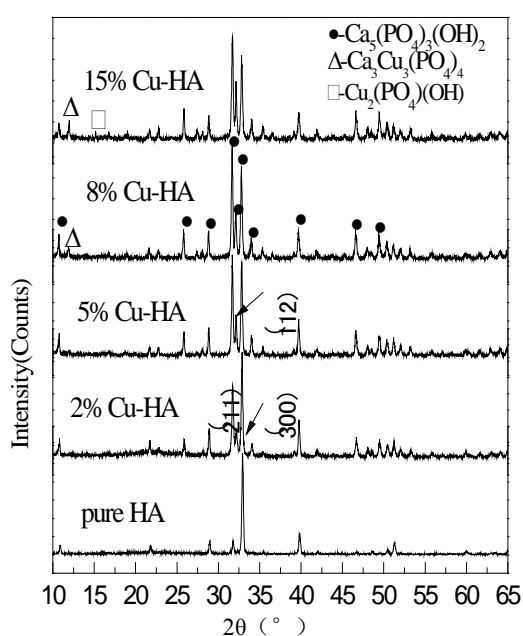


Fig.3 XRD patterns of Cu ions doped HA whiskers

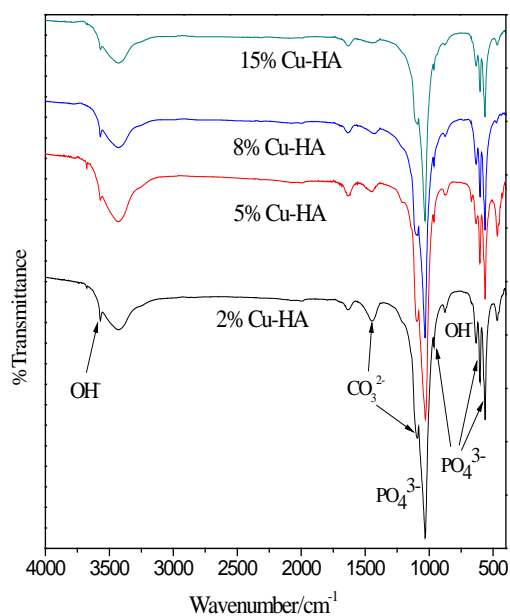


Fig.4 FTIR spectra of Cu ions doped HA whiskers

As shown in Fig.3, the phase composition of Cu^{2+} doped HA (Cu-HA) obviously changed with the ions doping concentration. For the samples with doping proportion being below 8mol%, the precipitates were identified as HA (PDF#:09-432). While increasing Cu concentration, the diffraction peaks of the samples became broader due to the substitution of Cu^{2+} for Ca^{2+} , and the diffraction peak for (211) obviously became stronger, while (300) became weaker, showing a decreased the peak intensity ratio of $I_{(300)}/I_{(211)}$. These indicated that the Cu ions doping would impair the crystallinity of Cu-HA and affected the morphology of the crystals. Further increasing the Cu/(Ca+Cu) molar ratio more than 8%, the apatite structure was no longer sustained and the new phase, $\text{Ca}_3\text{Cu}_3(\text{PO}_4)_4$ (PDF#:72-203) for 8% Cu doping ions and $\text{Cu}_2(\text{PO}_4)(\text{OH})$ (PDF#:72-462) for 15% Cu, were appeared in the products.

The results of XRD pattern was also supported by FTIR spectra. It can be seen from Fig.4, the absorption bands for the stretching and bending of phosphate were recorded at 1092, 1030, 962, 633, 563 cm^{-1} and the absorption peaks for the stretching mode of hydroxyl group of HA were at 3570 and 633 cm^{-1} . Absorption peaks at 1448, 1092 cm^{-1} , assigned as CO_3^{2-} group, were also visible due to the synthesis being conducted in air at ambient temperature. In addition, the absorption peaks for OH^- and PO_4^{3-} became weaker and widen with the addition of Cu concentration, which was related to the

low crystallinity of Cu-HA caused by Cu^{2+} substitution in the HA crystal structure. The results of FIRT powerfully verified the analysis results of XRD.

Summary

Sr and Cu ions doped HA whiskers were successfully synthesized using hydrothermal homogeneous precipitation in a moderate acid solution. Ca^{2+} was partially substituted by Sr^{2+} or Cu^{2+} , but increasing the Sr or Cu doping concentration, the lattice distortion of the HA crystal occurred and their crystallinity was reduced. The second phase ($\text{Ca}_3(\text{PO}_4)_2$) appeared when doping proportion of Sr-HA was above 20mol%. For Cu substitution, $\text{Ca}_3\text{Cu}_3(\text{PO}_4)_4$ and $\text{Cu}_2(\text{PO}_4)(\text{OH})$ appeared when Cu doping proportion was above 8mol% and 15mol%, respectively. To obtain highly crystallized and pure HA whiskers, the upper doping proportion of Sr-HA was estimated at 20mol%, and for Cu-HA was at 8mol%.

Acknowledgement

This work was supported by National Nature Science Foundation of China (No.51372182) and the Fundamental Research Funds for the Central Universities (No. 2011-IV-133)

References

- [1] H. Q. Zhang, M. Zhang and L. W. Fu: Key. Eng. Mater Vol. 531-532 ((2013), p. 250
- [2] O. L. Ming, X. F. Liu and L. Huang: J. Mater. Sci: Mater. 19 (2008), p. 799
- [3] I. Mayer, J. D. B. Featherstone: J. Cryst. Growth. 66 (2000), p. 2
- [4] I. Cacciottia, A. Bianco, M. Lombardi: J. Eur. Ceram. Soc. 29 (2009), p. 2969
- [5] R. Z. Legeros, J. P. Legeros, in: Phosphate Minerals, Edited by J. O. Nriagu and P. B. Moore Springer Velag, NY (1984)
- [6] R. Z. Legeros: Monogr. Oral. Sci. 15 (1990), p. 154
- [7] S. Koutsopoulos: J. Biomed. Mater. Res. 62 (2002), p. 601
- [8] I. V. Fadeev, L. I. Shvorneva and S. M. Barinov: Inorg. Mater Vol. 39 (2003), p. 1103
- [9] E. J. Underwood, in: Trace Elements in Human and Animal Nutrition, edited by Walter Mertz, NY (1982)
- [10] F. Z. Ren, R. L. Xin and X. Ge: Acta. Biomater. 5 (2009), p. 3142
- [11] Z. H. Li, J. M. Wu and S. J. Huang: J. Inorg. Mater. 26 (2011), p. 51
- [12] T. N. Kim, Q. L. Feng and J. Kim: J. Mater Sci: Mater. 9 (1998), p. 130
- [13] H. Q. Zhang, B. W. Darvell: Acta. Biomater. 6 (2010), p. 3218